Applied Catalysis B: Environmental 147 (2014) 677–683

Contents lists available at ScienceDirect

Applied Catalysis B: Environmental

journal homepage: www.elsevier.com/locate/apcatb

Kinetic investigation of the catalytic conversion of cellobiose to sorbitol

Leila Negahdar[a], Jens U. Oltmanns[a], Stefan Palkovits[b], Regina Palkovits[a,*]

[a] Institut für Technische und Makromolekulare Chemie, RWTH Aachen University, Aachen, Germany
[b] Center for Molecular Transformations, RWTH Aachen University, Aachen, Germany

ARTICLE INFO

Article history:
Received 11 July 2013
Received in revised form
23 September 2013
Accepted 28 September 2013
Available online 8 October 2013

Keywords:
Cellobiose
Sorbitol
Catalytic system
Hydrolysis
Hydrogenation
Kinetics

ABSTRACT

The reaction pathway and the kinetics of the conversion of cellobiose to sorbitol catalyzed by silicotungstic acids combined with ruthenium supported on activated carbon were studied. Two competing reaction pathways starting from cellobiose could be confirmed. The conversion of cellobiose either follows the hydrolysis to glucose or it passes through a hydrogenation of cellobiose to cellobitol (3-β-D-glucopyranosyl-D-glucitol). Cellobitol is subsequently hydrolyzed to sorbitol and glucose. At moderate temperatures of 393 K cellobitol becomes the main product with a maximum selectivity of 81%. Raising the reaction temperature to 443 K decreases the cellobitol selectivity to 1% while the maximum sorbitol selectivity increases to 75%. Kinetic modeling shows activation energies of 115 and 69 kJ mol^{-1} for the hydrolysis of cellobiose and subsequent hydrogenation of glucose. For cellobitol formation followed by hydrolysis 76 and 103 kJ mol^{-1} can be determined together with overall higher reaction rates at lower temperatures.

1. Introduction

In recent years concerns about depletion of fossil fuel reserves, increasing energy demand and global challenges have motivated our society to look for alternative sources of energy and feedstocks for chemical industry. Biomass is a highly promising alternative carbon source which is renewable and potentially sustainable [1–3]. Among all types of biomass cellulose is the most widespread non-edible polysaccharide and is considered to be one of the main feedstocks for sustainable fuel and chemical production. However, valorization of cellulose is still challenging due to its robust crystalline structure and insolubility in conventional solvents [4–9]. Most processes suffer from high energy consumption and low chemical selectivity. Therefore, designing more selective and efficient catalytic systems for the conversion of cellulose to platform chemicals is highly desirable. Especially combining molecular acids with supported metal catalysts provides a promising opportunity for the conversion of cellulose into value-added chemicals such as sorbitol [10]. Sorbitol is used as precursor in food and pharmaceutical industry and as platform chemical for the synthesis of chemical compounds such as isosorbide, sorbitan, glycerol, L-sorbose, etc [11]. Additionally, a further transformation of sorbitol into alkanes as well as efficient aqueous phase reforming for hydrogen generation have been demonstrated [12,13].

Recently several studies have reported the catalytic conversion of cellulose into sorbitol. A catalytic system containing molecular acids such as H_2SO_4, HCl or heteropoly acids combined with supported metal catalysts like Pt, Pd and Ru could efficiently catalyze the conversion of cellulose to sorbitol [10,14,15]. The highest yield of sugar alcohols (81%) could be achieved by the combination of heteropoly acids with supported ruthenium catalysts [14]. Previous studies focused on the design of efficient catalytic systems for the conversion of cellulose to sorbitol in order to maximize productivity. However, only a few mechanistic investigations are available [16] and a complete kinetic model describing the catalytic conversion of cellulose to sorbitol is still missing. Mechanistic studies and reaction kinetics can provide an insight into the reaction pathway and help to identify key intermediate compounds in the reaction network. Such studies allow a quantitative description of the effects of reaction conditions on reaction rates and the selectivity of the desired products. Therefore, a kinetic analysis may help to improve the catalytic performance and to rationalize process development.

The aim of this work is to gain insights into the reaction mechanism and kinetics of the catalytic conversion of cellobiose to sorbitol. Cellulose is a polymer with a very complex molecular structure driving a detailed kinetic study of its transformation difficult. Therefore, studying simple model molecules of cellulose such as cellobiose presents a promising possibility. Cellobiose represents

* Corresponding author. Tel.: +49 241 8026497.
E-mail address: Palkovits@itmc.rwth-aachen.de (R. Palkovits).

0926-3373/$ – see front matter © 2013 Elsevier B.V. All rights reserved.
http://dx.doi.org/10.1016/j.apcatb.2013.09.046

Nomenclature

a	liquid-solid interface area ($m^2\ m^{-3}$)
C	concentration ($mol\ m^{-3}$)
$C^*_{H_2}$	solubility of hydrogen in the liquid ($mol\ m^{-3}$)
Ca	Carberry number
C_b	concentration in bulk liquid ($mol\ m^{-3}$)
d_p	catalyst particle diameter (m)
d_s	stirring diameter (m)
D	diffusion coefficient ($m^2\ s^{-1}$)
D_e	effective diffusion coefficient ($m^2\ s^{-1}$)
E_a	activation energy ($kJ\ mol^{-1}$)
$k_{i,0}$	pre-exponential constant (s^{-1})
K	adsorption constant ($m^3\ mol^{-1}\ kg_{cat}^{-1}$)
k_La	volumetric gas–liquid mass transfer coefficient (s^{-1})
k_{LS}	liquid–solid mass transfer coefficient ($m\ s^{-1}$)
k_i	reaction rate coefficient (s^{-1})
n	reaction order
N_s	stirring speed (s^{-1})
N_p	power number
P	pressure (Pa)
P_2	pressure after absorption state (Pa)
P_1	pressure before saturation state (Pa)
P_0	pressure at initial state before absorption (Pa)
r_{obs}	observed volumetric reaction rate ($mol\ (m^3\ s)^{-1}$)
R	ideal gas constant ($Pa\ m^3\ (mol\ K)^{-1}$)
t	time (s)
T	temperature (K)
S_p	catalyst particle external surface area (m^2)
V_L	volume of liquid (m^3)
V_p	catalyst particle volume (m^3)

Dimensionless numbers

Re	Reynolds number
Sc	Schmidt number
Sh	Sherwood number

Greek letters

η_i	internal catalyst effectiveness factor
η_e	external catalyst effectiveness factor
μ_L	dynamic viscosity of the liquid ($kg\ (m\ s)^{-1}$)
ρ_L	density of the liquid ($kg\ m^{-3}$)
ϕ	Thiele modulus
Φ	Weisz modulus

the basic repeating unit of cellulose and consists of two glucose monomers linked by a β(1–4) glycosidic bond (Fig. 1).

The presented study focusses on the kinetics of the hydrolytic hydrogenation of cellobiose to sorbitol with a catalytic system consisting of heteropoly acids and a supported ruthenium catalyst (5 wt.% Ru/C). Furthermore, possible reaction pathways and key intermediate compounds of this reaction are discussed. In the kinetic study the effects of mass transfer on the hydrogenation reaction are evaluated and kinetic models covering different reaction temperatures are developed.

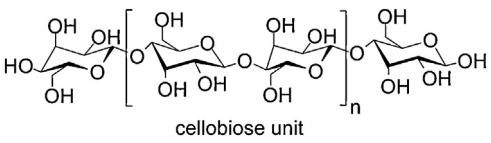

Fig. 1. Structure of cellulose and cellobiose.

2. Materials and methods

The experiments were carried out in a 50 ml stainless steel batch autoclave equipped with a sampling valve. The autoclave was loaded with 1.17 mmol cellobiose, 0.175 g heteropoly acid (silicotungstic acid), 0.1 g Ru/C (5 wt.%) and 20 ml of water. The reactor was then purged and vented with N_2 and H_2 at room temperature. The pressure was immediately adjusted to the experimental conditions. The reactor was then preheated under hydrogen pressure to the desired temperature and operated at a pressure range of 3.5–5 MPa and at 393–463 K for 3 h. At various time intervals liquid samples were taken and analyzed off-line using an HPLC (Shimadzu LC-10A) with a RI-detector. Separation of the components was achieved by an organic acid resin column (CS-Chromatographie, Germany, 300 mm × 8.0 mm and 100 mm × 8.0 mm) operated at 313 K. The eluent (154 μl of CF_3COOH in 1 l of water) was supplied at the 1 ml min^{-1} flow rate. Chemicals such as cellobiose, sorbitol, heteropoly acid (HPA, silicotungstic acid) and 5 wt.% Ru/C were purchased from Sigma-Aldrich. Cellobitol (3-β-D-glucopyranosyl-D-glucitol) was self-synthesized and characterized by ^{13}C NMR spectroscopy.

3. Results and discussion

3.1. Mechanistic study of hydrolytic hydrogenation of cellobiose

Numerous studies have reported the hydrolytic hydrogenation of cellulose or cellobiose to sorbitol to follow a cleavage of the glycosidic (C–O–C) bonds via hydrolysis and consecutive hydrogenation of glucose to sorbitol [17–19]. However, our experimental results of the cellobiose conversion to sorbitol indicate an additional reaction pathway to occur. We were able to emphasize that in the presence of a molecular acid and a supported metal catalyst cellobiose either undergoes hydrolysis to glucose or as an alternative pathway proceeds through a hydrogenation of the C–O bond on one of the glucose rings leading to cellobitol (3-β-D-glucopyranosyl-D-glucitol). In a subsequent reaction cellobitol can undergo hydrolysis to sorbitol and glucose. The proposed reaction pathways of the conversion of cellobiose are illustrated in Scheme 1.

Only few studies discuss the formation of cellobitol during the transformation of cellobiose. Therein, Kuo et al. reported the formation of cellobitol under neutral and basic conditions applying ruthenium nanoclusters in the ionic liquid 1-butyl-3-methylimidazolium chloride [20]. However, they concluded that the formation of cellobitol was not related to sorbitol formation. Instead, sorbitol was formed via direct hydrogenolysis of the β(1,4)-glycosidic bond of cellobiose under such conditions delivering sorbitol and dideoxyhexitol. A first study discussing cellobitol as intermediate in the transformation of cellobiose to sorbitol has been presented by Wang et al. [16]. They observed cellobitol in the conversion of cellobiose over carbon nanotube-supported Ru catalysts in neutral aqueous solutions and concluded that the formation of cellobitol followed by hydrolysis is the main pathway for sorbitol formation. Recently, Makkee et al. investigated the reaction mechanism of the transformation of cellobiose into sorbitol in aqueous $ZnCl_2$ with Ru/C as hydrogenation catalyst [21]. Their experimental data pointed towards a competition of two reaction pathways, (1) via cellobitol formation followed by hydrolysis and (2) via hydrolysis of cellobiose and subsequent hydrogenation. Under the presented reaction conditions path (1) was kinetically most important. Nevertheless, they suggested that various parameters such as reaction temperature, catalyst loading as well as the

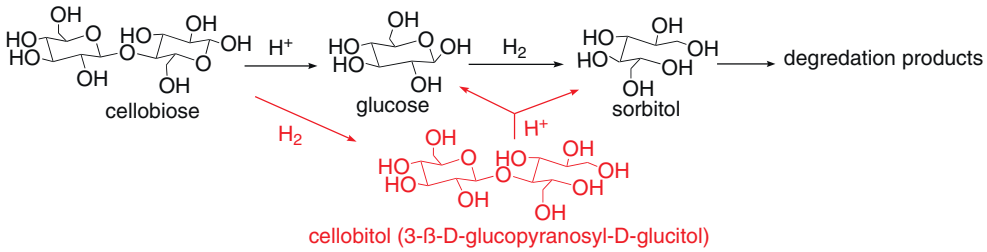

Scheme 1. Proposed reaction pathways for the conversion of cellobiose with HPA and Ru/C.

addition of mineral acids may influence the relative contribution of both pathways.

We herein present a kinetic investigation determining reaction rates and main activation energies of these competing reaction paths. The study confirms indeed that both pathways occur and their relative contribution strongly depends on the selected reaction conditions. Fig. 2 shows time resolved product selectivity courses at different reaction temperatures. Selectivity is defined as molar ratio of the respective product $n_{product}$ with regard to the consumed amount of cellobiose ($n_{Cellobiose,0} - n_{Cellobiose,t}$) at time t (ESI). At moderate temperatures of 393 K cellobitol is the main product with a maximum selectivity of 81%. Increasing the reaction temperature up to 443 K decreases the cellobitol selectivity to less than 1% after 1.25 h reaction time while the selectivity of sorbitol rises to a maximum of 75%. These observations suggest a simultaneous hydrolysis of cellobitol to sorbitol and glucose. However, comparing both time resolved datasets of the cellobiose conversion with HPA and Ru/C the presence of two competing reaction pathways with different intermediate substrates becomes obvious. At lower temperatures of up to 413 K the hydrogenation of the C–O bond at one of the glucose rings of cellobiose seems to be dominant while for higher temperatures direct hydrolysis of cellobiose becomes favorable.

Dependent on the reaction conditions cellobitol seems to play a key role as an intermediate compound in the catalytic hydrogenation of cellobiose. To gain insight into the thermochemistry of the two reaction pathways and to enable a kinetic modeling, experiments with cellobitol as substrate appear necessary. In line, cellobitol was synthesized and isolated. It can be produced selectively in neutral water at 433 K yielding 99% cellobitol after ca. 2 h (Fig. 3). At higher temperatures such as 463 K cellobitol undergoes consecutive reactions to sorbitol and further degradation reactions via dehydration as well as C–C and C–O bond cleavage occur.

Other possible side reactions, e.g. via dehydration of released glucose to form 5-hydroxymethylfurfural and levulinic acid as well as humin formation were not observed under our reaction conditions. This is due to a sufficiently high hydrogenation activity of the metal catalyst resulting in a fast hydrogenation of glucose to

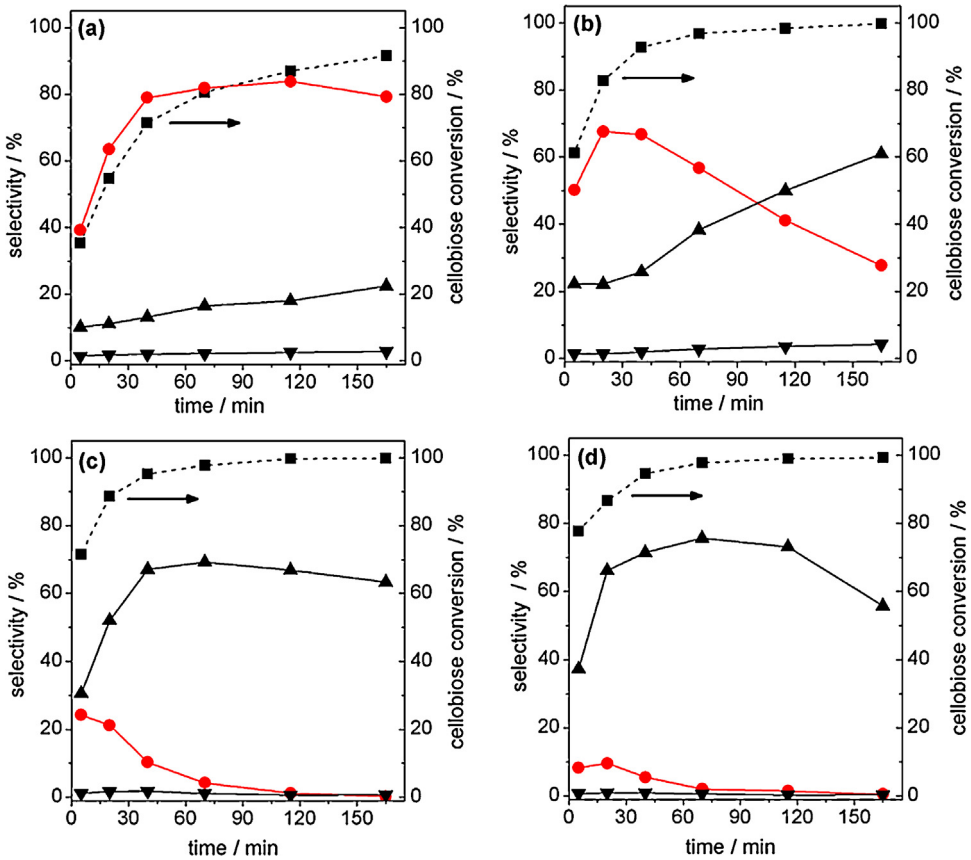

Fig. 2. Selectivity of cellobitol (●), glucose (▼), sorbitol (▲) and cellobiose conversion (■) as a function of elapsed time (a) 393, (b) 413, (c) 433 and (d) 443 K, Reaction conditions: cellobiose, 1.17 mmol; Ru/C, 0.1 g; HPA, 0.175 g; H_2O, 20 cm^3; H_2, 5 MPa; time, 2.5 h.

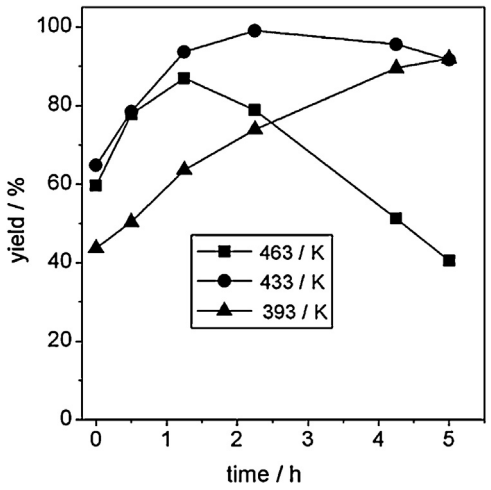

Fig. 3. Yield of Cellobitol as a function of elapsed time, Reaction conditions: cellobiose, 1.17 mmol; Ru/C, 0.1 g; H_2O, 20 cm^3; H_2, 5 MPa.

sorbitol. Under all mentioned reaction conditions only a low yield of glucose was observed as the hydrogenation of glucose to sorbitol takes place on the metal catalyst with high selectivity and rate [22]. Our previous investigation on sorbitol dehydration under comparable reaction condition emphasized as well the absence of the described degradation reactions via glucose dehydration and humin formation [23].

3.2. Kinetic study on the catalytic conversion of cellobiose to sorbitol

3.2.1. Mass transfer effects

Kinetic experiments were performed in a batch autoclave. To study the intrinsic kinetics of this three-phase system it is crucial to carry out the experiments in the absence of mass transfer limitations [24] which are typically examined by varying the stirring speed or the catalyst particle size. To study for example the effect of gas–liquid mass transfer on the catalytic reaction the stirring speed is increased until the reaction rate remains constant [25]. Therefore to check whether gas-liquid mass transfer is controlling the reaction the stirrer speed was varied between 600 and 1200 rpm. There was a negligible difference in the reaction rates indicating the absence of gas–liquid mass transfer limitations (Fig. S1). Additionally literature criteria can be used to verify the absence of mass transfer limitations. For example the absence of external mass transfer can be checked using the Carberry number being a dimensionless number representing the ratio of the observed reaction rate to the maximum transfer rate (Eqs. (1) and (2)). In general for first order reactions the absence of transfer limitations is verified if the value of the resulting effectiveness factor is above 0.95 [25].

$$Ca_{G-L} = \frac{r_{obs}}{k_L a C^*_{H_2}} \quad (1)$$

$$\eta_e = (1 - Ca)^n \quad (2)$$

To calculate a Carberry number according to equation (1) the maximum transfer rate was calculated by using the volumetric gas-liquid mass transfer coefficient and the hydrogen solubility. The volumetric gas-liquid mass transfer coefficient (k_La) of H_2 for the calculation was determined using the pressure step method [26].

The hydrogen solubility ($C^*_{H_2}$) was taken based on data published by Pray et al. [27]. Combining these data the influence of mass transfer was estimated for the initial reaction conditions. The detailed calculations to verify the absence of mass transfer limitation can be found in the Supporting Information. Table 1 shows the calculated results indicating with an effectiveness factor η above 0.95 in all cases that mass transfer limitations can be neglected for the used reaction conditions.

Table 1
Evaluation of the absence/presence of transport limitations.[a]

T (K)	P (Mpa)	Ca_{G-L}	n_{G-L}	Ca_{L-S}	n_{L-S}	ϕ_{H_2}	η_{H_2}
373	5	0.0028	0.99	0.0019	0.99	0.0034	0.99
393	5	0.0036	0.99	0.0025	0.99	0.0047	0.99

[a] Reaction conditions: cellobiose, 1.17 mmol; Ru/C, 0.1 g; H_2O, 20 cm^3.

To verify the absence of liquid–solid mass transfer limitation a Carberry type equation can be used which now contains liquid–solid mass transfer coefficient (k_{LS}) (Eq. (3)).

$$Ca_{L-S} = \frac{r_{obs}}{k_{LS} a C_b} \quad (3)$$

The required liquid–solid mass transfer coefficient was estimated by a typical correlation of the Sherwood number Sh for slurry reactors [28].

$$Sh = \frac{k_{LS} d_p}{D} = 2 + 0.4 Re^{1/4} Sc^{1/3} \quad (4)$$

In case of internal mass transfer limitations the catalyst particles size is a decisive factor, therefore small catalyst particles are used in order to eliminate internal resistances. For the used carbon supported ruthenium catalyst the average particle diameter was in the order of 19 μm, leading to an ignorable internal diffusion resistance. Furthermore, the Weisz modulus being the ratio of the observed reaction rate and the maximum effective rate of diffusion was used to evaluate the absence of internal diffusion limitations (Eqs. (5) and (6)) [29].

$$\Phi = \left(\frac{V_p}{S_p}\right)^2 \left(\frac{n+1}{2}\right) \frac{r_{obs}}{D_e C_b} \quad (5)$$

$$\Phi = \eta_i \phi^2 \quad (6)$$

From the values reported in Table 1 it can be concluded that in all examined cases the mass transport resistance is negligible and it can be assumed that the experiments are carried out in the intrinsic regime.

In this kinetic study a low concentration of cellobiose was used and in the studied pressure range Henry's law is valid leading to a hydrogen concentration in the solution proportional to the applied hydrogen pressure. Investigating the effect of the hydrogen pressure on the initial rate of cellobiose the hydrogen pressure dependency approaches a saturation situation at pressures above 3.5 MPa at low cellobiose concentrations (Fig. S2). However, in highly concentrated cellobiose solutions the low solubility of hydrogen may cause diffusion limitations. Based on the aforementioned experimental observations a kinetic control of the reaction can safely be assumed at a stirrer speed above 750 rpm, a hydrogen pressure above 3.5 MPa and low concentrations of cellobiose in solution. The kinetic modeling of the reaction network was therefore undertaken under these experimental conditions.

3.2.2. Kinetic modeling

Scheme 2 illustrates the possible reaction pathways of the catalytic conversion of cellobiose to sorbitol. The pathway can be divided into two main catalytic reactions including hydrolysis of cellobiose (k_1) or cellobitol (k_3) and hydrogenation of cellobiose (k_2) or glucose (k_4). Possible side reactions of sorbitol to by-products are further hydrogenolysis (k_7 and k_8) and dehydration

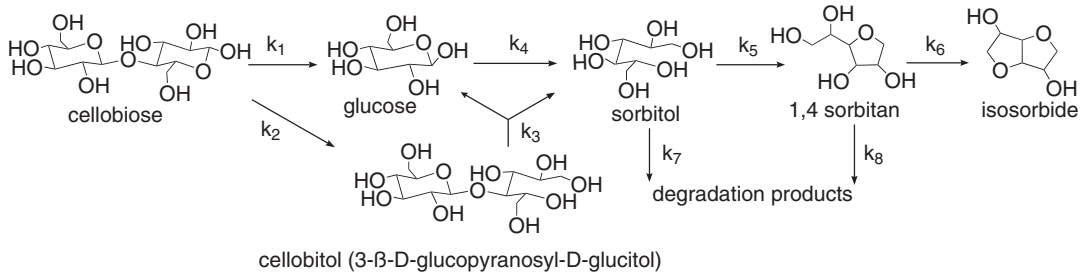

Scheme 2. Schematic illustration of the reaction network for the catalytic conversion of cellobiose to sorbitol.

reactions (k_5 and k_6). By-products formed by dehydration of glucose such as 5-hydroxymethylfurfural and levulinic acid were not found under the applied reaction conditions.

Several kinetic studies on acid-catalyzed hydrolysis of cellulosic biomass have been reported in literature. A first kinetic study of biomass hydrolysis was determined by Saeman in 1945 [30]. Most of the other kinetic studies on hydrolysis of cellulose followed the kinetic model developed earlier by Saeman with the assumption of a pseudo first order reaction for the hydrolysis [31–33]. The reaction rate constants in this study follow a modified form of the Arrhenius equation including the temperature effects (T) and the acid concentration (A). This equation has been further generalized by replacing the acid concentration with the hydrogen ion concentration in solution.

$$k_i = k_{i,0}\left[H^+\right]^m e^{-E/RT},\ i = 1, 2 \tag{7}$$

Herein k_0 represents the pre-exponential factor (s^{-1}), [H^+] is the hydrogen ion concentration in solution and m is an empirical exponent [34].

For the development of our kinetic models for the hydrogenation reactions it was assumed that no catalyst deactivation is taking place during the reaction and the adsorption of the solvent and the products on the catalyst surface is negligible. For hydrogenation reactions the Langmuir–Hinshelwood–Hougen–Watson (LHHW) model can be assumed with a non-competitive adsorption of hydrogen and cellobiose or glucose at different sites of the catalyst (Eq. (8)) [35].

$$r = \frac{kK_{\text{cellobiose}}C_{\text{cellobiose}}K_{H_2}P_{H_2}}{1 + K_{\text{cellobiose}}C_{\text{cellobiose}}} \tag{8}$$

On the basis of the preliminary kinetic analysis some simplifications can be made. At the selected operation conditions a large excess of hydrogen and a low concentration of cellobiose and glucose is present in solution leading to the assumption of the reaction to be pseudo first - order (Eq. (9)).

$$r = k_2 C_{\text{cellobiose}} \tag{9}$$

The constant k_2 is a lumped parameter including the intrinsic rate constant as well as adsorption constant. The dehydration reactions are also assumed to be first-order [23,36]. Based on the reaction network illustrated in Scheme 2 the following ordinary differential equations (ODEs) can be proposed for the individual components as a function of time:

$$\frac{d\left(C_{\text{cellobiose}}\right)}{dt} = -k_1 C_{\text{cellobiose}} - \frac{m_{\text{cat}}}{V_L} k_2 C_{\text{cellobiose}} \tag{10}$$

$$\frac{d\left(C_{\text{cellobitol}}\right)}{dt} = \frac{m_{\text{cat}}}{V_L} k_2 C_{\text{cellobiose}} - k_3 C_{\text{cellobitol}} \tag{11}$$

$$\frac{d\left(C_{\text{gulcose}}\right)}{dt} = 2k_1 C_{\text{cellobiose}} + k_3 C_{\text{cellobitol}} - \frac{m_{\text{cat}}}{V_L} k_4 C_{\text{glucose}} \tag{12}$$

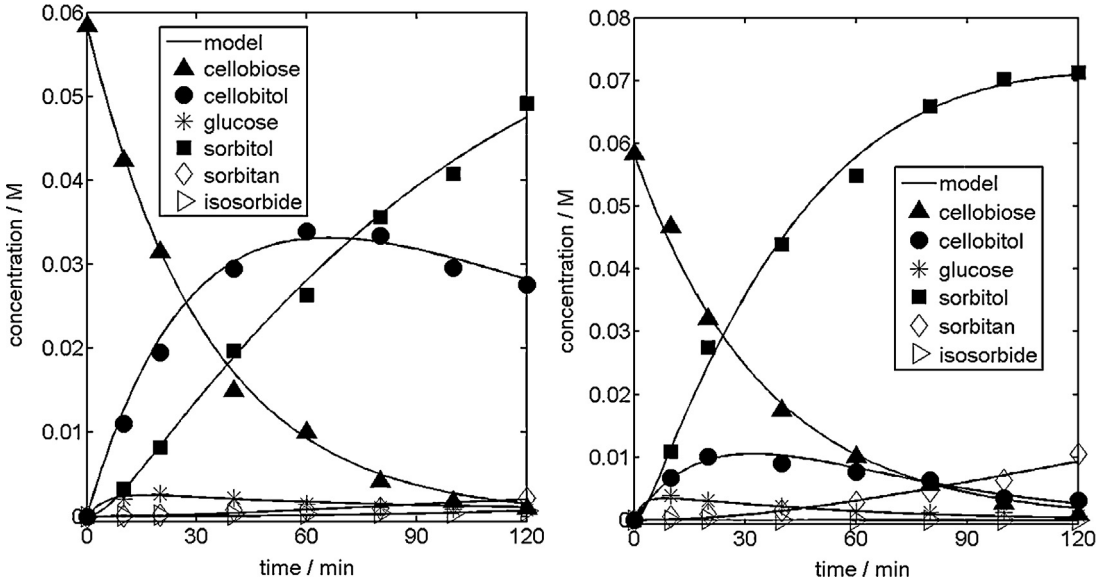

Fig. 4. Fit of the kinetic model (Eqs. (10) and (15)) to the experimental data; Reaction conditions: cellobiose, 1.17 mmol; Ru/C, 0.1 g; HPA, 0.175 g; H_2O, 20 cm^3; H_2, 5 MPa at (left) 423 K and (right) 443 K.

Table 2
Kinetic parameters for the catalytic conversion of cellobiose to sorbitol.

	Reaction T (K)				Activation energy (kJ mol^{-1})	R^2
	393	423	443	463		
k_1* (10^{-2} min^{-1})	0.014	0.319	1.013	2.98	115	0.98
k_2* (10^{-2} min^{-1})	0.119	0.717	2.183	3.76	76	0.98
k_3* (10^{-2} min^{-1})	0.032	0.551	1.785	3.51	103	0.97
k_4* (10^{-2} min^{-1})	0.203	1.911	3.574	4.74	69	0.92
k_5* (10^{-2} min^{-1})		0.010	0.024	0.48	164	0.93
k_6* (10^{-2} min^{-1})		0.001	0.027	0.084	178	0.94

* Parameters defined in Scheme 2.

$$\frac{d(C_{sorbitol})}{dt} = \frac{m_{cat}}{V_L}\left(k_4 C_{glucose} - k_7 C_{sorbitol}\right) + k_3 C_{cellobitol} + k_5 C_{sorbitol} \quad (13)$$

$$\frac{d(C_{sorbitan})}{dt} = k_5 C_{sorbitol} - \frac{m_{cat}}{V_L} k_8 C_{sorbitan} - k_6 C_{sorbitan} \quad (14)$$

$$\frac{d(C_{isosorbide})}{dt} = k_6 C_{sorbitan} \quad (15)$$

Matlab was used for the numerical integration of the ODEs and parameter estimations and moreover to compare the experimental data with the proposed kinetics. The rate constants and activation energies were estimated at different temperatures (393–463 K). Fig. 4 shows the curve fitting for the experimental data at 413 and 433 K. Further temperatures are available in the supplementary information (ESI, Fig. S5).

Table 2 summarizes the estimated values of the reaction rate constants and the corresponding activation energies. At temperatures below 463 K the rate constant k_2 (cellobiose to cellobitol) is significantly higher compared to the rate constant k_1 (cellobiose to glucose) indicating the hydrogenation step to proceed faster than hydrolysis. With increasing reaction temperature the rate constants of both reaction pathways become comparable and both reactions compete with each other.

Additionally, at temperatures below 463 K the rate constants of both hydrolysis steps (k_1 and k_3) are lower compared to the ones of the hydrogenation reactions (k_2 and k_4) reflecting the fact that hydrolysis is the rate-determining step independent of the reaction pathway. Nevertheless, a previous transformation of cellobiose to cellobitol appears to facilitate subsequent hydrolysis resulting in superior rate constant for the hydrolysis of cellobitol k_3 compared to cellobiose k_1. Overall the reaction rate constant k_4 for the hydrogenation of glucose to sorbitol is the highest compared with the other ones emphasizing a fast hydrogenation of glucose and explaining the low glucose concentrations detected under most reaction conditions. The rate constants of the subsequent dehydration of sorbitol to sorbitan (k_5) and further to isosorbide (k_6) are small corresponding to the low detected concentrations of these degradation products under the selected reaction conditions. These low concentrations hampered a kinetic modeling of further degradation reactions of sorbitan and isosorbide (k_7 and k_8). Nevertheless, values reported for corresponding activation energies of step 5 and 6 (164 and 178 kJ mol^{-1}) are in the same range as literature data reported recently for an acid free transformation in hot water (127 and 195 kJ mol^{-1}) [36].

Fig. 5 shows the the Arrhenius diagram of the reaction rate constants. Estimation of the activation energy of cellobiose hydrolysis E_1 yields a value of 115 kJ mol^{-1} which is in good agreement with the respective literature data (108–119 kJ mol^{-1}) [34,37,38].

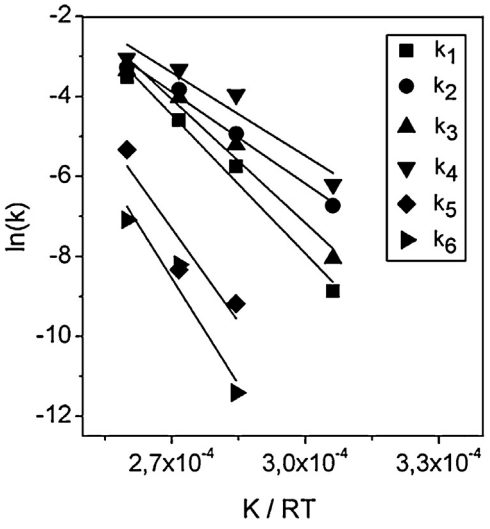

Fig. 5. Arrhenius diagram of the reaction rate constants for the estimations of activation energies of the catalytic conversion of cellobiose to sorbitol.
Schemes:

The activation energy E_3 for the hydrolysis of cellobitol was determined to be 103 kJ mol^{-1} which is lower than E_1 pointing out that the hydrolysis of cellobitol is easier compared to cellobiose under the used reaction conditions. The activation energy for the hydrogenation of glucose E_4 was estimated to 69 kJ mol^{-1} being also in good agreement with reported data ranging from 55 to 71 kJ mol^{-1} [35,39]. An activation energy E_2 of 76 kJ mol^{-1} can be determined for the hydrogenation of cellobiose to cellobitol corresponding well to the data for glucose hydrogenation. For the modified Arrhenius equation (Eq. (7)) the values of the empirical exponent m were estimated to be 1.02 and 0.96 respectively.

Overall, analysis of the reaction network emphasizes two reaction pathways delivering sorbitol based on cellobiose. Considering the fact that subsequent dehydration and hydrogenolysis of sorbitol need to be suppressed to achieve high selectivities of sorbitol, a preferential transformation via cellobitol formation appears interesting. The facilitated hydrolysis of cellobitol compared to cellobiose (E_a and k) enables a reaction under neutral or weakly acidic reaction conditions at rather low reaction temperatures. Moreover, preliminary results indicate a second ring hydrogenation of cellobitol overcoming glucose as reaction intermediate. Current investigations adress the impact of these finding on the transformation of cellulose via metal catalyzed hydrogenation and hydrogenolysis reactions.

A direct transfer of the obtained data to cellulose is certainly difficult especially considering the crystalline structure of cellulose. However recent studies on a selective depolymerization of cellulose to cello-oligomers could provide the base of a controlled sorbitol production via the selective hydrogenation of such oligomers under optimized reaction conditons [40,41].

4. Conclusions

Our mechanistic study on the hydrolytic hydrogenation of cellobiose to sorbitol confirms two competing reaction pathways starting from cellobiose. Cellobiose either undergoes hydrolysis to glucose or hydrogenation to cellobitol (3-β-D-glucopyranosyl-D-glucitol). Cellobitol can then be further hydrolyzed to glucose and sorbitol. Cellobitol can be produced selectively with up to 99% yield utilizing a Ru/C catalyst in neutral water and appropriate reaction conditions. To evaluate the absence of mass transfer limitations literature criteria were applied to ensure the kinetic experiments being performed in the intrinsic regime. Kinetic parameters of both reaction pathways were obtained from the proposed model with non-linear regression analysis. The results emphasize hydrolysis as rate determining step independent of the reaction pathway. Overall, a selective transformation of cellobiose to sorbitol proceeding via cellobitol formation appears possible. Especially at lower reaction temperature this reaction pathway dominates and overall lower activation energies together with higher rate constants can be observed.

Acknowledgements

We acknowledge financial support by the Robert Bosch Foundation in the frame of the Robert Bosch Junior Professorship for the efficient utilization of renewable resources. This work was performed as part of the Cluster of Excellence "Tailor-Made Fuels from Biomass" funded by the Excellence Initiative by the German federal and state governments to promote science and research at German universities.

Appendix A. Supplementary data

Supplementary data associated with this article can be found, in the online version, at http://dx.doi.org/10.1016/j.apcatb.2013.09.046.

References

[1] P. McKendry, Bioresource Technol. 83 (2002) 37–46.
[2] B. Kamm, P.R. Gruber, M. Kamm, Biorefineries - Industrial Processes and Products, Wiley-VCH Verlag GmbH & Co, KGaA, Weinheim, 2006.
[3] G.W. Huber, S. Iborra, A. Corma, Chem. Rev. 106 (2006) 4044–4098.
[4] H. Kobayashi, A. Fukuoka, Green Chem. 15 (2013) 1740–1763.
[5] R. Rinaldi, F. Schüth, ChemSusChem. 2 (2009) 1096–1107.
[6] J.A. Geboers, S. Van de Vyver, R. Ooms, B. Op de Beeck, P.A. Jacobs, B.F. Sels, Catal. Sci. Technol. 1 (2011) 714–726.
[7] S. Van de Vyver, J. Geboers, P.A. Jacobs, B.F. Sels, ChemCatChem. 3 (2011) 82–94.
[8] S. Dumitriu, Polysaccharides: Structural Diversity and Functional Versatility, second ed., Marcel Dekker, New York, 2005.
[9] D. Klemm, B. Heublein, H.P. Fink, A. Bohn, Angew. Chem. Int. Ed. 44 (2005) 3358–3393.
[10] R. Palkovits, K. Tajvidi, J. Procelewska, R. Rinaldi, A. Ruppert, Green Chem. 12 (2010) 972–978.
[11] A.M. Ruppert, K. Weinberg, R. Palkovits, Angew. Chem. Int. Ed. 51 (2012) 2564–2601.
[12] G. de Wit, J.J. de Vlieger, A.C. Kock-van Dalen, R. Heus, R. Laroy, A.J. van Hengstum, A.P.G. Kieboom, H. van Bekkum, Carbohydr. Res. 91 (1981) 125–138.
[13] A.P.G. Kieboom, J.F. De Kreuk, H. Van Bekkum, J. Catal. 20 (1971) 58–66.
[14] R. Palkovits, K. Tajvidi, A.M. Ruppert, J. Procelewska, Chem. Commun. 47 (2011) 576–578.
[15] J. Geboers, S. Van de Vyver, K. Carpentier, K. de Blochouse, P. Jacobs, B. Sels, Chem. Commun. 46 (2010) 3577–3579.
[16] W.P. Deng, M. Liu, X.S. Tan, Q.H. Zhang, Y. Wang, J. Catal. 271 (2010) 22–32.
[17] A. Fukuoka, P.L. Dhepe, Angew. Chem. Int. Ed. 45 (2006) 5161–5163.
[18] (a) G.F. Liang, C.Y. Wu, L.M. He, J. Ming, H.Y. Cheng, L.H. Zhuo, F.Y. Zhao, Green Chem. 13 (2011) 839–842;
(b) B. Op de Beeck, J. Geboers, S. Van de Vyver, J. Van Lishout, J. Snelders, W.J.J. Huijgen, C.M. Courtin, P.A. Jacobs, B.F. Sels, ChemSusChem. 6 (2013) 199–208.
[19] P.L. Dhepe, A. Fukuoka, ChemSusChem. 1 (2008) 969–975.
[20] N. Yan, C. Zhao, C. Luo, P.J. Dyson, H.C. Liu, Y. Kou, J. Am. Chem. Soc. 128 (2006) 8714–8715.
[21] J. Li, H.S.M.P. Soares, J.A. Moulijn, M. Makkee, Catal. Sci. Technol. 3 (2013) 1540–1546.
[22] B. Kusserow, S. Schimpf, P. Claus, Adv. Synth. Catal. 345 (2003) A102.
[23] J.U. Oltmanns, S. Palkovits, R. Palkovits, Appl. Catal. A 456 (2013) 168–173.
[24] F. Kapteijn, J.A. Moulijn, R.A. van Santen, R. Wever, Stud. Surf. Sci. Catal. 123 (1999) 81–106.
[25] C.N. Satterfield, Cc/Eng. Tech. Appl. Sci. (1979) E10.
[26] E. Dietrich, C. Mathieu, H. Delmas, J. Jenck, Chem. Eng. Sci. 47 (1992) 3597–3604.
[27] H.A. Pray, C.E. Schweickert, B.H. Minnich, Ind. Eng. Chem. 44 (1952) 1146–1151.
[28] N.Y.Y. Sano, T. Adachi, J. Chem. Eng. Jpn. 7 (1974) 255.
[29] R. Dittmeyer, G. Emig, Handbook of Heterogeneous Catalysis, Wiley-VCH Verlag GmbH & Co. KGaA, 2008.
[30] J.F. Saeman, Ind. Eng. Chem. 37 (1945) 43–52.
[31] R.D. Fagan, H.E. Grethlei, A.O. Converse, A. Porteous, Environ. Sci. Technol. 5 (1971) 545.
[32] J.P. Franzidis, A. Porteous, J. Anderson, Resour. Conserv. Recycl. 5 (1982) 215–225.
[33] D.R. Thompson, H.E. Grethlein, Ind. Eng. Chem. Prod. Res. Dev. 18 (1979) 166–169.
[34] N.S. Mosier, C.M. Ladisch, M.R. Ladisch, Biotechnol. Bioeng. 79 (2002) 610–618.
[35] E. Crezee, B.W. Hoffer, R.J. Berger, M. Makkee, F. Kapteijn, J.A. Moulijn, Appl. Catal. A 251 (2003) 1–17.
[36] A. Yamaguchi, N. Hiyoshi, O. Sato, M. Shirai, Green Chem. 13 (2011) 873–881.
[37] L. Vanoye, M. Fanselow, J.D. Holbrey, M.P. Atkins, K.R. Seddon, Green Chem. 11 (2009) 390–396.
[38] B.M. Kabyemela, M. Takigawa, T. Adschiri, R.M. Malaluan, K. Arai, Ind. Eng. Chem. Res. 37 (1998) 357–361.
[39] R.S.J. Wisniak, Ind. Eng. Chem. Prod. Res. Dev. 18 (1979) 50.
[40] N. Maine, R. Rinaldi, F. Schüth, ChemSusChem. 5 (2012) 1449–1454.
[41] J. Hilgert, N. Meine, R. Rinaldi, F. Schüth, Energy Environ. Sci. 6 (2013) 92–96.